

# Synthesis and Characterisation of Bis(diphenylphosphino)-amine Complexes of Platinum(II) †

Pravat Bhattacharyya, Richard N. Sheppard, Alexandra M. Z. Slawin, David J. Williams and J. Derek Woollins\*

Department of Chemistry, Imperial College, South Kensington, London SW7 2AY, UK

The complexes  $[\text{PtCl}(\text{PR}_3)(\text{dppa})]\text{Cl}$  ( $\text{PR}_3 = \text{PMe}_3, \text{PMe}_2\text{Ph}, \text{PMePh}_2, \text{PBU}^n, \text{PPh}_3$  or  $\text{PEt}_3$ ) have been prepared by the reaction of bis(diphenylphosphino)amine,  $\text{dppa}$  ( $\text{Ph}_2\text{PNHPPH}_2$ ), with *cis*- $[\text{PtCl}_2(\text{PR}_3)_2]$  in  $\text{CH}_2\text{Cl}_2$ . With  $[\text{PtCl}_2(\text{dppe})]$  ( $\text{dppe} = \text{Ph}_2\text{PCH}_2\text{CH}_2\text{PPh}_2$ ),  $[\text{Pt}(\text{dppe})(\text{dppa})]\text{Cl}_2$  is formed. The  $\text{PEt}_3$  complex undergoes halide exchange with excess of  $\text{Br}^-$  or  $\text{I}^-$  to give  $[\text{PtX}(\text{PEt}_3)(\text{dppa})]\text{X}$ . The compound  $[\text{PtCl}_2(\text{dppa})]$  has been prepared from  $[\text{PtCl}_2(\text{cod})]$  ( $\text{cod} = \text{cycloocta-1,5-diene}$ ). The products have been characterised by  $^{31}\text{P}\{-^1\text{H}\}$ ,  $^{195}\text{Pt}$  and  $^1\text{H}$  NMR spectroscopy, microanalysis and FAB mass spectrometry. The molecular structures of  $[\text{PtCl}(\text{PMe}_2\text{Ph})(\text{dppa})]\text{Cl}\cdot 1.5\text{CHCl}_3$ ,  $[\text{PtCl}(\text{PBU}^n_3)(\text{dppa})]\text{Cl}$  and  $[\text{Pt}(\text{dppe})(\text{dppa})]\text{Cl}_2\cdot\text{CH}_2\text{Cl}_2$  have been determined by single-crystal X-ray diffraction, and show a square-planar arrangement around the platinum with the  $\text{dppa}$  acting as a chelate through both phosphorus atoms to give a four-membered  $\text{PtP}_2\text{N}$  ring whose geometry is distinctly different from that of the deprotonated systems. All of the  $\text{dppa}$  NH groups hydrogen bond to an adjacent  $\text{Cl}^-$  in the solid state.

Although the co-ordination chemistry of bis(diphenylphosphino)methane,  $\text{Ph}_2\text{PCH}_2\text{PPh}_2$  ( $\text{dppm}$ )<sup>1</sup> has been the subject of substantial interest, the chemistry of  $\text{dppa}$ ,  $\text{Ph}_2\text{PNHPPH}_2$ , which is isoelectronic, is relatively poorly developed. Recent work has focused upon the co-ordination chemistry of  $[\text{Ph}_2\text{PNPPH}_2]^-$  and the related anion  $[\text{Ph}_2\text{P}(\text{E})\text{NP}(\text{E})\text{Ph}_2]^-$  ( $\text{E} = \text{O}, \text{S}$  or  $\text{Se}$ ).<sup>2-4</sup> However, few platinum complexes containing  $\text{dppa}$  or its *N*-substituted derivatives have been prepared.<sup>5-10</sup> These types of compounds are of interest because of their potential as catalysts for the oligomerisation and polymerisation of alkenes. Here we report on the reaction of  $\text{dppa}$  with *cis*- $[\text{PtCl}_2(\text{PR}_3)_2]$  which proceeds, for monodentate phosphines, with displacement of one molecule of phosphine and one chloride anion to give complexes in which  $\text{dppa}$  forms a four-membered chelate ring with the platinum. In the case of  $[\text{PtCl}_2(\text{dppe})]$  ( $\text{dppe} = \text{Ph}_2\text{PCH}_2\text{CH}_2\text{PPh}_2$ ),  $[\text{Pt}(\text{dppe})(\text{dppa})]\text{Cl}_2$  is formed. Structural and spectroscopic data for the complexes are presented.

## Experimental

**General.**—All syntheses involving *cis*- $[\text{PtCl}_2(\text{PR}_3)_2]$  were performed under an atmosphere of oxygen-free nitrogen using standard Schlenk techniques. The metathesis reactions were performed in an air using a dried reflux condenser fitted with a  $\text{CaCl}_2$  drying tube. Dichloromethane was dried and distilled over  $\text{CaH}_2$  under nitrogen. Hexane, AnalaR acetone,  $\text{CDCl}_3$  (98%) and diethyl ether were used as received. Both NaI and KBr were of reagent grade. Bis(diphenylphosphino)amine ( $\text{dppa}$ ) was prepared according to the literature method.<sup>11</sup> Proton (89.6 MHz),  $^{31}\text{P}\{-^1\text{H}\}$  (109.4 and 202.5 MHz) and  $^{195}\text{Pt}$  NMR (57.9 MHz) spectra were recorded ( $\text{CDCl}_3$  solution) on JEOL FX90Q, JEOL JNM EX270 and Bruker AM500 FT spectrometers. Infrared spectra were recorded as KBr discs on a Perkin Elmer 1720X FT spectrometer. Microanalyses were carried out by the Imperial College Microanalytical Service, FAB mass spectra were recorded on a VG 7070E machine.

**Preparation of the Complexes.**— $[\text{PtCl}(\text{PR}_3)(\text{dppa})]\text{Cl}$  ( $\text{PR}_3 = \text{PMe}_3$  **1**,  $\text{PMe}_2\text{Ph}$  **2**,  $\text{PMePh}_2$  **3**,  $\text{PBU}^n_3$  **4**,  $\text{PPh}_3$  **5** or  $\text{PEt}_3$  **6**). A typical synthesis was performed as follows, for  $\text{PR}_3 = \text{PPh}_3$ . The compounds *cis*- $[\text{PtCl}_2(\text{PPh}_3)_2]$  (93 mg, 0.117 mmol) and  $\text{dppa}$  (47 mg, 0.122 mmol) were stirred for 30 min in  $\text{CH}_2\text{Cl}_2$  (15  $\text{cm}^3$ ) at room temperature. The solvent was removed *in vacuo* and the  $^{31}\text{P}$  NMR spectrum of the crude product mixture recorded in  $\text{CDCl}_3$ . The complex was recrystallised to give colourless crystals by slow diffusion of hexane into the  $\text{CDCl}_3$  solution. Yields were typically > 70%.

$[\text{PtX}(\text{PEt}_3)(\text{dppa})]\text{X}$  ( $\text{X} = \text{Br}$  **7** or  $\text{I}$  **8**). The compound  $[\text{PtCl}(\text{PEt}_3)(\text{dppa})]\text{Cl}$  **6** (23 mg, 0.03 mmol) and KBr or NaI (0.40 mmol) were suspended in acetone (10  $\text{cm}^3$ ) and refluxed with stirring for 90 min. After cooling to room temperature the solvent was removed under reduced pressure. The solid was washed on a sinter funnel with distilled water (4  $\times$  10  $\text{cm}^3$ ) and diethyl ether (2  $\times$  10  $\text{cm}^3$ ), and air dried. Yield of crude product ca. 75%.

$[\text{Pt}(\text{dppe})(\text{dppa})]\text{Cl}_2\cdot\text{CH}_2\text{Cl}_2$  **9**. The compounds  $[\text{PtCl}_2(\text{dppe})]$  (94 mg, 0.14 mmol) and  $\text{dppa}$  (55 mg, 0.14 mmol) were stirred for 30 min. in  $\text{CH}_2\text{Cl}_2$  (10  $\text{cm}^3$ ) at room temperature. The solvent was removed *in vacuo* and the  $^{31}\text{P}$  NMR spectrum of the crude product mixture recorded. The complex was recrystallised as pale green crystals from dichloromethane upon addition of hexane. Yield 65%.

$[\text{PtCl}_2(\text{dppa})]$  **10**. The compounds  $[\text{PtCl}_2(\text{cod})]$  ( $\text{cod} = \text{cycloocta-1,5-diene}$ ) (379 mg, 1.0 mmol) and  $\text{dppa}$  (389 mg, 1.0 mmol) were placed in a Schlenk tube and  $\text{CH}_2\text{Cl}_2$  (10  $\text{cm}^3$ ) was added. The suspension was stirred for 3 h at room temperature. The white solid was filtered off and washed with dichloromethane (10  $\text{cm}^3$ ), methanol (10  $\text{cm}^3$ ), dichloromethane (10  $\text{cm}^3$ ) and air dried. Yield 97%.

Microanalytical data for the complexes are presented in Table 1. Proton,  $^{31}\text{P}\{-^1\text{H}\}$  and  $^{195}\text{Pt}$  NMR and IR data for the complexes are compiled in Tables 2 and 3.

**X-Ray Crystallography.**—Slow diffusion of hexane into solutions of the appropriate complex gave crystals of  $[\text{PtCl}(\text{PMe}_2\text{Ph})(\text{dppa})]\text{Cl}\cdot 1.5\text{CHCl}_3$  **2**,  $[\text{PtCl}(\text{PBU}^n_3)(\text{dppa})]\text{Cl}$  **4** and  $[\text{Pt}(\text{dppe})(\text{dppa})]\text{Cl}_2\cdot\text{CH}_2\text{Cl}_2$  **9** suitable for X-ray analysis.

† Supplementary data available: see Instructions for Authors, *J. Chem. Soc., Dalton Trans.*, 1993, Issue 1, pp. xxiii–xxviii.

**Table 1** Microanalytical data for the complexes, with calculated values in parentheses

Complex	Analysis (%)		
	C	H	N
1 [PtCl(PMe <sub>3</sub> )(dppa)]Cl	42.70 (44.60)	3.65 (4.15)	1.70 (1.95)
2 [PtCl(PMe <sub>2</sub> Ph)(dppa)]Cl*	47.15 (48.70)	3.75 (4.10)	1.65 (1.75)
3 [PtCl(PMePh <sub>2</sub> )(dppa)]Cl·2CHCl <sub>3</sub>	42.35 (42.95)	3.10 (3.35)	1.25 (1.30)
4 [PtCl(PBu <sup>n</sup> <sub>3</sub> )(dppa)]Cl	50.30 (50.65)	5.45 (5.65)	1.70 (1.65)
5 [PtCl(PPh <sub>3</sub> )(dppa)]Cl·2CHCl <sub>3</sub>	45.70 (45.85)	3.60 (3.35)	1.20 (1.20)
6 [PtCl(PEt <sub>3</sub> )(dppa)]Cl	46.85 (46.80)	4.90 (4.70)	1.65 (1.80)
9 [Pt(dppe)(dppa)]Cl <sub>2</sub> ·CH <sub>2</sub> Cl <sub>2</sub>	52.85 (54.00)	4.05 (4.15)	1.15 (1.25)
10 [PtCl <sub>2</sub> (dppa)]	43.50 (44.25)	2.90 (3.25)	1.95 (2.15)

\* This compound showed varying degrees of solvation.

**Table 2** <sup>31</sup>P-{<sup>1</sup>H} NMR data for complexes 1–8<sup>a</sup>

	δ(P)			<sup>1</sup> J(Pt–P)/Hz			<sup>2</sup> J(P–P)/Hz		
	P(1)	P(2)	P(3)	P(1)	P(2)	P(3)	P(1)–P(2)	P(1)–P(3)	P(2)–P(3) <sup>b</sup>
1	9.2	3.2	–13.1	1953	3090	2367	52	421	–8
2	7.8	1.7	–7.1	2003	3096	2371	51	419	–9
3	6.1	0.9	6.6	2120	3094	2320	50	400	–5
4	9.45	2.5	9.3	2020	3157	2380	59	424	–5
5	3.3	0.2	20.3	2100	3120	2423	49	412	–5
6	9.3	2.9	17.8	1967	3135	2352	50	400	–10
7	7.6	2.6	15.6	1932	3143	2346	47	399	–9
8	2.1	–2.5	11.8	1884	3041	2368	49	395	–7

<sup>a</sup> Atoms P(1) and P(2) are on the dppa ligand, P(3) is *trans* to P(1). <sup>b</sup> Computer simulations of the spectra are relatively insensitive to the magnitude of this coupling constant.

**Table 3** <sup>195</sup>Pt-{<sup>1</sup>H} NMR, <sup>1</sup>H NMR and IR data for complexes 1–10

Complex	δ( <sup>195</sup> Pt)	δ(NH)	<sup>3</sup> J(Pt–NH)/Hz	ν(NH)/cm <sup>–1</sup>
1	–4336	11.72	167	2736
2	–4324	11.75	173	2712
3	–4315	11.75	173	2704
4	–4306	11.70	170	2703
5	–4297	11.75	168	2793
6	–4322	11.75	164	2708
7	–4475	11.03	168	2777
8	–4761	10.10	177	3227
9	–4765	11.70	130	2801
10*	—	—	—	3209

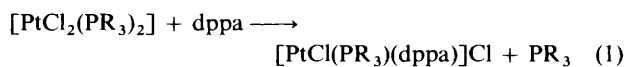
\* Lack of solubility of 10 in common organic solvents prevented measurement of NMR spectra.

Details of the data collections and refinements are given in Table 4. In all three structures the N–H proton was located from a Δ*F* map and refined isotropically subject to an N–H distance constraint; all of the remaining hydrogen atoms were placed at idealised positions, assigned isotropic thermal parameters and allowed to ride on the parent carbon atoms. All three structures were solved by direct methods and refined by full-matrix least-squares methods using the SHELXTL PC system.<sup>12</sup>

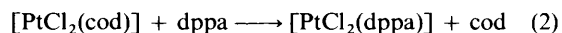
Additional material available from the Cambridge Crystallographic Data Centre comprises H-atom coordinates, thermal parameters and remaining bond lengths and angles.

## Results and Discussion

The reaction between dppa and *cis*-[PtCl<sub>2</sub>(PR<sub>3</sub>)<sub>2</sub>] in CH<sub>2</sub>Cl<sub>2</sub> proceeds according to equation (1). Conversion is quantitative



by <sup>31</sup>P NMR spectroscopy. An analogous substitution of phosphine and halide has been reported for the reaction between Li(PPh<sub>2</sub>YPPH<sub>2</sub>) (Y = CH or N) and [MX<sub>2</sub>(PR<sub>3</sub>)<sub>2</sub>] (M = Ni or Pd; X = Cl or Br; PR<sub>3</sub> = PPh<sub>3</sub>, PMe<sub>2</sub>Ph or PEt<sub>3</sub>).<sup>2</sup> Our results show that prior deprotonation of dppa is not necessary for a reaction with *cis*-[PtCl<sub>2</sub>(PR<sub>3</sub>)<sub>2</sub>] to occur, and that products of similar structure to the above nickel and palladium complexes can be obtained. The reaction of [PtCl<sub>2</sub>(dppe)] with dppa proceeds to give [Pt(dppe)(dppa)]Cl<sub>2</sub> quantitatively, the chelate effect being sufficient for displacement of both chlorides to occur in preference to phosphine. The chloride ligand of [PtCl(PEt<sub>3</sub>)(dppa)]Cl 6 is labile, and the corresponding bromide (7) and iodide (8) derivatives can be prepared by metathesis with an excess of the appropriate halide ion in refluxing acetone. The reaction reverses when the complexes are left to stand in CHCl<sub>3</sub> solution over several days at room temperature due to halide exchange with traces of HCl in the solvent. Complex [PtCl<sub>2</sub>(dppa)] 10 was prepared by the reaction of dppa with [PtCl<sub>2</sub>(cod)] in CH<sub>2</sub>Cl<sub>2</sub> [equation (2)];



the white solid separates from the reaction mixture immediately. However, the extreme insolubility of the product in any common organic solvent prevented measurement of the NMR or mass spectra. Thus only IR and microanalytical data could be obtained. Owing to the lack of solubility of [PtCl<sub>2</sub>(dppa)], attempts at chloride substitution have so far proved unsuccessful.

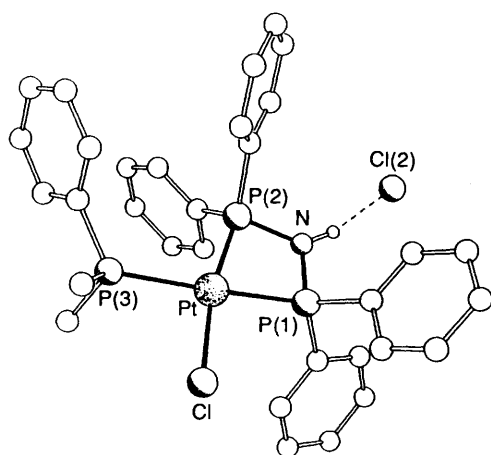
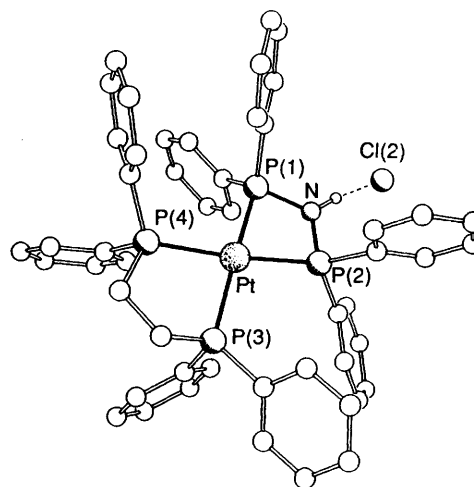
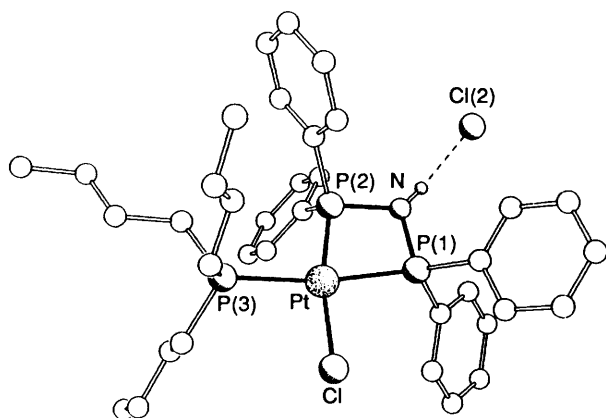
The reaction between [PtCl(PEt<sub>3</sub>)(dppa)]Cl 6 and dppa in CH<sub>2</sub>Cl<sub>2</sub> proceeds with displacement of the remaining chloride and phosphine to give the previously reported homoleptic complex [Pt(dppa)<sub>2</sub>]Cl<sub>2</sub>.<sup>7</sup> All of the complexes described here are air- and moisture-stable both in the solid state and in solution.

The crystal structures of complexes 2, 4 and 9 are shown in Figs. 1–3 respectively. Atomic coordinates are given in Tables 5–7 and selected bond lengths and angles in Table 8. Despite

**Table 4** Details of the data collection and refinements for compounds **2**, **4** and **9**

Compound	<b>2</b>	<b>4</b>	<b>9</b>
Empirical formula	C <sub>32</sub> H <sub>32</sub> Cl <sub>2</sub> NP <sub>3</sub> Pt·1.5CHCl <sub>3</sub>	C <sub>36</sub> H <sub>48</sub> Cl <sub>2</sub> NP <sub>3</sub> Pt	C <sub>50</sub> H <sub>45</sub> Cl <sub>2</sub> NP <sub>4</sub> Pt·CH <sub>2</sub> Cl <sub>2</sub>
Colour, habit	Clear, blocks	Clear, blocks	Green, plates
Crystal size/mm	0.32 × 0.48 × 0.34	0.54 × 0.32 × 0.22	0.24 × 0.36 × 0.38
Crystal system	Triclinic	Orthorhombic	Monoclinic
Space group	<i>P</i> $\bar{1}$	<i>Pna</i> 2 <sub>1</sub>	<i>P</i> 2 <sub>1</sub> / <i>n</i>
<i>a</i> /Å	9.607(2)	23.091(5)	12.027(3)
<i>b</i> /Å	15.350(4)	10.072(2)	21.979(6)
<i>c</i> /Å	16.739(5)	16.784(3)	18.168(3)
$\alpha$ /°	113.76(2)		
$\beta$ /°	100.76(2)		91.58(2)
$\gamma$ /°	102.04(2)		
<i>U</i> /Å <sup>3</sup>	2106	3903	4801
<i>Z</i>	2	4	4
<i>M</i>	968.5	853.7	1134.7
<i>D<sub>c</sub></i> /Mg m <sup>-3</sup>	1.527	1.453	1.570
Absorption coefficient/mm <sup>-1</sup>	3.88	3.879	3.315
<i>F</i> (000)	950	1712	2264
2 $\theta$ range/°	4–50	3–50	3–48
Independent reflections [ <i>R</i> <sub>int</sub> (%)]	7407 (0.00)	3558 (0.00)	7550 (2.07)
Observed reflections	6121 [ <i>F</i> > 4.0 $\sigma$ ( <i>F</i> )]	2652 [ <i>F</i> > 4.0 $\sigma$ ( <i>F</i> )]	6080 [ <i>F</i> > 3.0 $\sigma$ ( <i>F</i> )]
Absorption correction	Semi empirical	None	Semi empirical
Min., max. transmission	0.510, 0.770	—	0.261, 0.344
No. of parameters refined	368	343	458
Final <i>R</i> ( <i>R</i> ')	4.47 (3.83)	3.55 (3.35)	3.78 (3.54)
Largest and mean $\Delta$ / $\sigma$	0.009 and 0.001	0.014 and 0.001	0.012 and 0.001
Data/parameter ratio	16.6	7.7	13.3
Largest difference peak, hole/e Å <sup>-3</sup>	1.24, -1.00	1.05, -0.48	0.83, -0.86

Details in common: Siemens P<sub>4</sub> diffractometer; Mo-K $\alpha$  radiation ( $\lambda$  = 0.71073 Å); weighting scheme,  $w^{-1} = \sigma^2(F) + 0.0005F^2$ .

**Fig. 1** Crystal structure of [PtCl(PMe<sub>2</sub>Ph)(dppa)]Cl·1.5CHCl<sub>3</sub> **2****Fig. 3** Crystal structure of [Pt(dppe)(dppa)]Cl<sub>2</sub>·CH<sub>2</sub>Cl<sub>2</sub> **9** showing the hydrogen-bonded chloride; the non-hydrogen bonded chloride is omitted for clarity.**Fig. 2** Crystal structure of [PtCl(PBu<sub>3</sub>)(dppa)]Cl **4**

the difference in the nature of the phosphine co-ligands, the molecules have essentially identical cores. These comprise the central platinum atom in a distorted square-planar geometry co-ordinated by bidentate dppa with, in **2** and **4**, PR<sub>3</sub> and Cl<sup>-</sup> as the other ligands and in **9** dppe. There are small deviations from planarity in the platinum co-ordination. In compound **2** the Pt–P(1)–P(2)–P(3)–Cl plane shows a maximum deviation of 0.065 Å (for Pt) with the nitrogen atom lying 0.13 Å from this plane; in **4** the maximum deviation is 0.04 Å (for Pt) with the nitrogen atom 0.23 Å from the plane. Interestingly, in compound **9** the co-ordination plane is noticeably more distorted with P(1) being 0.13 Å and N being 0.31 Å from the plane. The major distortion is actually at P(3) and this atom lies 0.46 Å from the Pt–P(1)–P(2)–P(4) plane (which is coplanar to within 0.03 Å). In all three cases the deviation of the nitrogen atom from the co-ordination plane is due to a folding along the

**Table 5** Atomic coordinates ( $\times 10^4$ ) with estimated standard deviations in parentheses (e.s.d.s) for compound **2**

Atom	x	y	z	Atom	x	y	z
Pt	1477(1)	486(1)	3803(1)	C(17)	-2575	116	3178
Cl	3327(3)	769(2)	5093(2)	C(18)	-1983	364	2569
P(1)	2041(2)	2108(1)	4012(1)	C(19)	-1019(7)	-1026(4)	910(4)
N	767(7)	1790(4)	3038(4)	C(20)	-838	-1593	67
P(2)	-47(2)	560(1)	2668(1)	C(21)	433	-1251	-148
P(3)	865(3)	-1224(2)	3377(2)	C(22)	1525	-343	481
Cl(2)	-348(3)	3177(2)	2356(2)	C(23)	1344	224	1325
C(1)	5010(7)	2323(5)	4130(7)	C(24)	72	-118	1539
C(2)	6377	2738	4043	C(25)	-2162(10)	-2108(6)	2667(6)
C(3)	6563	3521	3810	C(26)	-3488	-2776	1986
C(4)	5382	3891	3663	C(27)	-3451	-3414	1121
C(5)	4015	3476	3749	C(28)	-2088	-3384	938
C(6)	3829	2693	3982	C(29)	-762	-2715	1619
C(7)	2579(5)	3330(4)	5829(3)	C(30)	-799	-2077	2484
C(8)	2327	4031	6586	C(31)	734(14)	-1518(8)	4289(7)
C(9)	1191	4443	6460	C(32)	2332(15)	-1640(9)	3013(13)
C(10)	307	4154	5577	C(40)	7809(14)	5008(10)	7754(10)
C(11)	559	3453	4821	Cl(10)	6936(5)	4061(4)	6640(3)
C(12)	1695	3040	4947	Cl(20)	6515(5)	5495(4)	8226(4)
C(13)	-2890(7)	504(6)	1905(4)	Cl(30)	8814(8)	4599(4)	8393(5)
C(14)	-4389	395	1851	C(50)	-6933(18)	-3024(12)	-608(10)
C(15)	-4980	146	2459	Cl(40)	-6671(7)	-4124(4)	-971(3)
C(16)	-4073	7	3123	Cl(50)	-7084(12)	-2591(8)	430(4)
				Cl(60)	-5466(12)	-2072(11)	-381(13)

**Table 6** Atomic coordinates ( $\times 10^4$ ) with e.s.d.s in parentheses for compound **4**

Atom	x	y	z	Atom	x	y	z
Pt	9 207(1)	9 011(1)	8 021(1)	C(16)	9 156	3 742	6 698
Cl	9 555(2)	10 556(3)	8 960(2)	C(17)	8 988	5 067	6 622
P(1)	8 241(1)	8 979(4)	8 378(2)	C(18)	8 914	5 849	7 301
P(2)	8 723(1)	7 574(3)	7 265(2)	C(19)	8 905(4)	9 034(9)	5 898(5)
P(3)	10 153(1)	8 707(3)	7 574(2)	C(20)	8 791	9 418	5 115
N	8 102(3)	7 715(9)	7 769(5)	C(21)	8 356	8 787	4 682
C(1)	8 064(5)	9 449(9)	9 968(6)	C(22)	8 033	7 772	5 031
C(2)	7 818	9 204	10 712	C(23)	8 146	7 387	5 815
C(3)	7 502	8 042	10 841	C(24)	8 582	8 018	6 248
C(4)	7 433	7 126	10 226	C(25)	10 606(5)	7 997(18)	8 369(9)
C(5)	7 679	7 371	9 481	C(26)	10 439(7)	6 585(18)	8 586(10)
C(6)	7 994	8 532	9 352	C(27)	10 864(9)	5 989(22)	9 177(13)
C(7)	7 975(3)	11 639(8)	8 223(5)	C(28)	10 696(10)	4 563(29)	9 364(16)
C(8)	7 609	12 701	8 045	C(29)	10 247(5)	7 605(12)	6 746(7)
C(9)	7 055	12 462	7 744	C(30)	10 850(6)	7 357(15)	6 431(10)
C(10)	6 868	11 162	7 620	C(31)	10 895(7)	6 528(22)	5 720(13)
C(11)	7 234	10 100	7 797	C(32)	11 508(8)	6 251(20)	5 452(15)
C(12)	7 787	10 339	8 099	C(33)	10 522(5)	10 215(13)	7 291(9)
C(13)	9 006(4)	5 305(9)	8 055(5)	C(34)	10 347(5)	10 814(13)	6 488(9)
C(14)	9 173	3 980	8 130	C(35)	10 668(6)	12 109(16)	6 301(10)
C(15)	9 248	3 199	7 452	C(36)	10 537(8)	12 621(17)	5 463(11)
				Cl(2)	7 037(1)	6 031(4)	7 588(3)

P(1)···P(2) axis. The fold angles between the PtP<sub>2</sub> and P<sub>2</sub>N planes are 5, 10 and 11° for **2**, **4** and **9** respectively. The Pt–P bond lengths are normal for Pt<sup>II</sup> and comparison of the Pt–P(2) bond length for the three structures reveals the expected shortening (by *ca.* 0.09 Å) of this in **2** and **4** compared with **9** as a result of the difference in *trans* influence of Cl *versus* P (Table 8). Within the four-membered ring the P–N bond lengths are, as expected, consistently longer than in the related palladium complex which contains a deprotonated ligand.<sup>2</sup> Accompanying deprotonation in [PdCl(PET<sub>3</sub>)(Ph<sub>2</sub>PNPPPh<sub>2</sub>)] there is<sup>2</sup> a significant reduction of the P–N–P and P–M–P angles and a consequent reduction in the P···P distance (*ca.* 0.17 Å) compared with the equivalent dimensions in all three structures reported here. It is thus apparent that there is significantly less ring strain in complexes containing the neutral dppa ligand compared to those containing the deprotonated ligand. Although several crystal structures of complexes containing dppa in a bridging geometry have been determined,<sup>13–18</sup> fewer

structures in which dppa functions as a bidentate ligand through the phosphorus atoms have been reported.<sup>2,8,15</sup>

In all three structures there is a strong N–H···Cl hydrogen bond (N···Cl distances in the range 3.00–3.10 Å) between the imido proton and a chloride anion. There are no other significant intermolecular contacts between the cations and anions.

In the <sup>1</sup>P-{<sup>1</sup>H} NMR spectra (Table 2) for the monophosphine complexes **1–8**, P(1) resonates to high frequency of P(2) as a result of the greater *trans* influence of P(3) compared to the halide X. The chemical shift of P(3) is more variable than for P(1) and P(2), spanning a range of 30 ppm. Phosphorus-31 chemical shifts at low frequency are a feature associated with phosphine groups in four-membered rings as a consequence of distortion around the phosphorus atom.<sup>19</sup> This is reflected in the <sup>31</sup>P NMR spectra of **1–9** by co-ordination shifts to low frequency exceeding 30 ppm for the dppa relative to the free molecule ( $\delta$  42.1). However, the magnitude of the shift must

**Table 7** Atomic coordinates ( $\times 10^4$ ) with e.s.d.s in parentheses for compound **9**

Atom	x	y	z	Atom	x	y	z
Pt	1974(1)	3705(1)	2905(1)	C(23)	4585	4194	1217
P(1)	1303(1)	4529(1)	2241(1)	C(24)	4499	4021	1952
N	2571(4)	4753(2)	2012(3)	C(25)	4541(3)	3238(2)	4160(2)
P(2)	3427(1)	4310(1)	2527(1)	C(26)	5640	3237	4429
P(3)	2774(1)	2803(1)	3305(1)	C(27)	6365	2776	4223
P(4)	364(1)	3173(1)	3162(1)	C(28)	5992	2315	3750
Cl(1)	1979(1)	3896(1)	4713(1)	C(29)	4894	2315	3482
Cl(2)	3360(2)	5741(1)	927(1)	C(30)	4168	2777	3687
C(1)	108(3)	5611(2)	2356(2)	C(31)	3129(4)	2513(2)	1857(2)
C(2)	-488	6042	2748	C(32)	3075	2145	1232
C(3)	-608	5974	3505	C(33)	2638	1558	1275
C(4)	-132	5476	3870	C(34)	2256	1341	1944
C(5)	464	5045	3478	C(35)	2310	1709	2569
C(6)	584	5113	2721	C(36)	2747	2296	2525
C(7)	-605(3)	4480(2)	1322(2)	C(37)	1915(5)	2480(3)	4011(3)
C(8)	-1167	4353	658	C(38)	680(5)	2571(3)	3843(4)
C(9)	-578	4150	54	C(39)	-789(3)	3803(2)	4246(2)
C(10)	572	4074	115	C(40)	-1589	4216	4475
C(11)	1134	4201	779	C(41)	-2363	4454	3966
C(12)	545	4404	1383	C(42)	-2335	4279	3229
C(13)	3791(3)	4897(2)	3865(2)	C(43)	-1535	3866	3000
C(14)	4315	5322	4326	C(44)	-761	3628	3509
C(15)	5215	5657	4076	C(45)	-1197(3)	2410(2)	2502(2)
C(16)	5591	5566	3365	C(46)	-1729	2121	1906
C(17)	5067	5140	2904	C(47)	-1330	2196	1198
C(18)	4167	4805	3154	C(48)	-399	2559	1086
C(19)	5265(3)	3613(2)	2265(2)	C(49)	134	2848	1682
C(20)	6117	3378	1843	C(50)	-266	2773	2390
C(21)	6203	3552	1108	C(60)	3680(8)	4229(6)	-828(7)
C(22)	5437	3959	795	Cl(30)	3415(2)	3494(1)	-471(2)
				Cl(40)	2823(2)	4363(2)	-1588(2)

**Table 8** Selected bond lengths (Å) and angles (°) for compounds **2**, **4** and **9**

	<b>2</b>	<b>4</b>	<b>9</b>
Pt-P(1)	2.297(2)	2.312(3)	2.309(2)
Pt-P(2)	2.229(2)	2.227(3)	2.316(2)
Pt-P(3)	2.331(2)	2.330(3)	2.312(2)
Pt-P(4)	—	—	2.319(2)
Pt-Cl(1)	2.346(3)	2.356(4)	—
P(1)-N	1.662(7)	1.665(10)	1.666(5)
P(2)-N	1.680(6)	1.670(9)	1.681(5)
Mean P-C(aryl)	1.79	1.79	1.80
Mean P-C(alkyl)	1.78	1.81	—
P(1)-Pt-P(2)	70.0(1)	69.7(1)	69.5(1)
P(2)-Pt-P(3)	103.9(1)	101.7(1)	105.9(1)
P(3)-Pt-P(4)/Cl(1)	88.1(1)	89.0(1)	81.2(1)
Cl(1)/P(4)-Pt-P(1)	97.8(1)	99.5(1)	102.6(1)
Pt-P(1)-N	91.9(2)	92.1(3)	93.1(2)
Pt-P(2)-N	94.8(2)	95.0(3)	92.4(2)
P(1)-N-P(2)	102.1(4)	102.2(5)	103.9(3)
P(1)···P(2)	2.598(2)	2.595(4)	2.636(2)
N···Cl(2)	3.07	3.00	3.10
H(1)···Cl(2)	2.11	2.05	2.13
N-H(1)···Cl(2)	166	165	169

depend upon more than simple bond-angle distortions at the phosphorus atoms, as co-ordination shifts of less than 10 ppm have been observed in the  $^{31}\text{P}\{-^1\text{H}\}$  NMR spectra of platinum complexes containing *N*-alkylated dppa derivatives.<sup>9,10</sup>

The  $^{31}\text{P}\{-^1\text{H}\}$  NMR spectra of the crude reaction mixtures of complexes **1**–**3** show a rapid chemical exchange process between free and co-ordinated monophosphine, which at room temperature gives line broadening and obscures all  $^{31}\text{P}\{-^1\text{H}\}$  coupling. Crystallisation of the complex to remove the excess of phosphine is necessary to reveal the true spectrum. The exchange process was not studied further by variable-temper-

ature  $^{31}\text{P}\{-^1\text{H}\}$  NMR spectroscopy. Phosphine exchange does not occur for the crude reaction mixtures of any of the other complexes. For compound **6** this is due to oxidation of the displaced phosphine in solution whilst for **4** and **5** it is steric crowding at the platinum which must prevent exchange, since no oxidation is apparent by  $^{31}\text{P}$  NMR spectroscopy. The  $^{31}\text{P}\{-^1\text{H}\}$  NMR spectra of complexes **1**, **2** and **5**–**8** have first-order patterns consisting of three doublets of doublets, with satellites from coupling to  $^{195}\text{Pt}$ . Satisfactory computer simulation<sup>20</sup> of the spectra was achieved by using  $^2J[\text{P}(2)\text{--P}(3)]$  of opposite sign to  $^2J[\text{P}(1)\text{--P}(2)]$  and  $^2J[\text{P}(1)\text{--P}(3)]$  (Fig. 4). For **3** and **4** (Fig. 5) the *trans* phosphorus nuclei P(1) and P(3) have nearly coincident chemical shifts, which produces deceptively simple patterns in their  $^{31}\text{P}$  NMR spectra. At 109.4 MHz the spectra appears to consist of a doublet for P(1) and P(3) with a triplet to low frequency for P(2). At 202.5 MHz all of the couplings within the spectrum are observed. The  $^{195}\text{Pt}$  satellites for P(1) and P(3) appear as doublets whilst those for P(2) are seen as a doublet of doublets. The chemical shifts and *J* values quoted in Table 2 for **3** and **4** were obtained by simulation.<sup>20</sup> The  $^{31}\text{P}\{-^1\text{H}\}$  NMR spectrum of compound **9** (Fig. 6) is of the AA'XX' type, where A, A' represent the dppa phosphorus nuclei and X, X' the dpe chelate. Of the 20 possible lines for an AA'XX' spin system, only 12 are observed. The chemical shifts and  $^{195}\text{Pt}\text{--}^{31}\text{P}$  couplings can be measured directly from the spectrum [ $\delta(\text{P}_A)$  13.1,  $^1J(\text{Pt}\text{--P}_A)$  2154;  $\delta(\text{P}_X)$  46.9,  $^1J(\text{Pt}\text{--P}_X)$  2412 Hz]. Conventional analysis<sup>21</sup> of the spectrum reveals the magnitudes of the  $^{31}\text{P}\text{--}^{31}\text{P}$  coupling constants to be:  $J(\text{A}\text{--A}')\{J[\text{P}(1)\text{--P}(2)]\} = 58$ ,  $J(\text{X}\text{--X}')\{J[\text{P}(3)\text{--P}(4)]\} = 0$ ,  $J(\text{A}\text{--X}')\{^{\text{trans}}J[\text{P}(1)\text{--P}(3)]\} = 334$ ,  $J(\text{A}\text{--X})\{^{\text{cis}}J[\text{P}(1)\text{--P}(4)]\} = 9$  Hz. Computer simulation of the spectrum is in agreement with the algebraic treatment that  $J(\text{A}\text{--X})$  is of opposite sign to the other  $^{31}\text{P}\text{--}^{31}\text{P}$  couplings. It has been suggested that small bond angles at the platinum in the four-membered ring of Pt-dppm chelate complexes causes a reduction in  $^1J(^{195}\text{Pt}\text{--}^{31}\text{P})$  compared to unstrained Pt-dppe chelates.<sup>22</sup> A similar effect for Pt-dppa systems is illustrated in the spectra of **9**, where  $^1J(\text{Pt}\text{--P}_X)$  exceeds  $^1J(\text{Pt}\text{--P}_A)$  by 250 Hz,

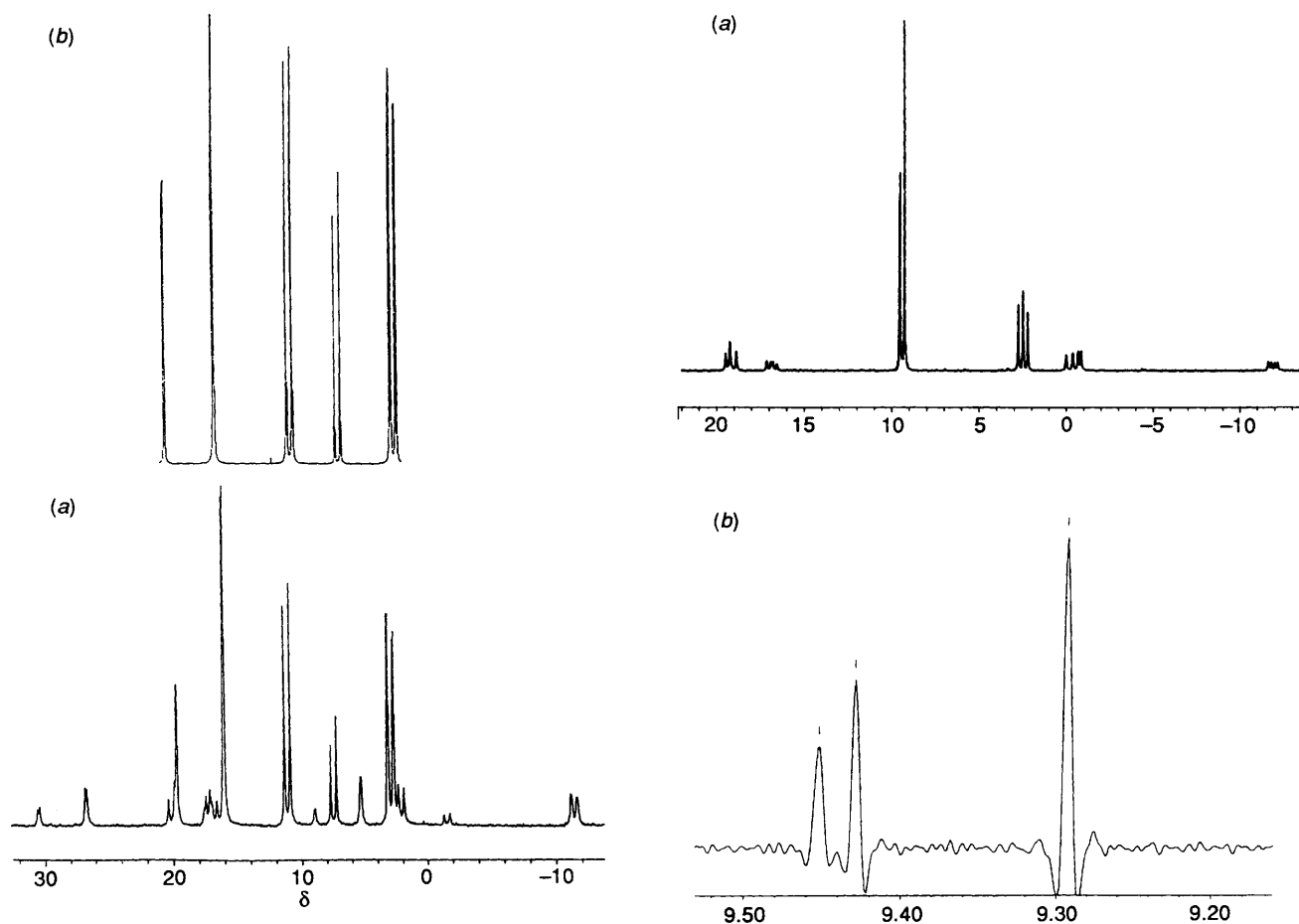


Fig. 4 (a)  $^{31}\text{P}\{-^1\text{H}\}$  NMR spectrum (109.4 MHz) and (b) simulation for  $[\text{PtCl}(\text{PEt}_3)(\text{dppa})]\text{Cl}$  6:  $^{195}\text{Pt}$  satellites omitted for clarity

while the crystal structure (see above) reveals P–Pt–P angles of  $81.2(1)$  and  $69.5(1)^\circ$  for the respective chelates. Similarly, for the monophosphine complexes  $^1J[\text{Pt-P}(3)]$  exceeds  $^1J[\text{Pt-P}(1)]$ . The reduction in  $^1J(\text{Pt-P})$  for the phosphorus atoms of the dppa chelate must arise from an increase in the proportion of p character in the Pt–P bond at the expense of s character. Further support for the assertion that P(1) and P(2) are coupled through both the platinum nucleus and the NH backbone of the dppa ligand is the comparison with complexes of formula  $[\text{PtCl}(\text{PR}_3)(\text{dppm})]\text{Cl}$  ( $\text{PR}_3 = \text{PBu}^n_3, \text{PEt}_3$  or  $\text{PPh}_2\text{Me}$ )<sup>23,24</sup> where the corresponding  $^2J(\text{P-P})$  coupling is found to be 65–70 Hz.

The  $^{195}\text{Pt}\{-^1\text{H}\}$  NMR spectra of compounds 1, 2 and 5–8 consists of eight lines of approximately equal intensity from the splitting of the platinum resonance by the three inequivalent phosphorus nuclei although for 3 and 4 the spectra consist of six main lines and four weaker lines, reflecting the second-order distortions observed in the  $^{31}\text{P}$  NMR spectra (Fig. 7). The spectrum of 9 is a triplet of triplets, due to coupling of the platinum to the two different pairs of phosphorus nuclei (Fig. 8). Shifts to high frequency in the  $^{195}\text{Pt}$  NMR spectra are a feature associated with platinum in four-membered rings,<sup>19</sup> although the lack of  $^{195}\text{Pt}$  NMR data for Pt–dppa complexes makes meaningful comparison of chemical shifts difficult. For the chloride complexes 1–6 there is a shift to higher frequency in the platinum resonance with increasing cone angle<sup>25</sup> of the phosphine (Fig. 9). This deshielding of the platinum nucleus as the bulk of the phosphine increases may arise from bond-angle distortions and/or Pt–P bond lengthening, with consequent weakening of that bond. An argument based upon purely steric grounds does not account for the difference in chemical shift between complexes 4 and 6, for which the phosphines have

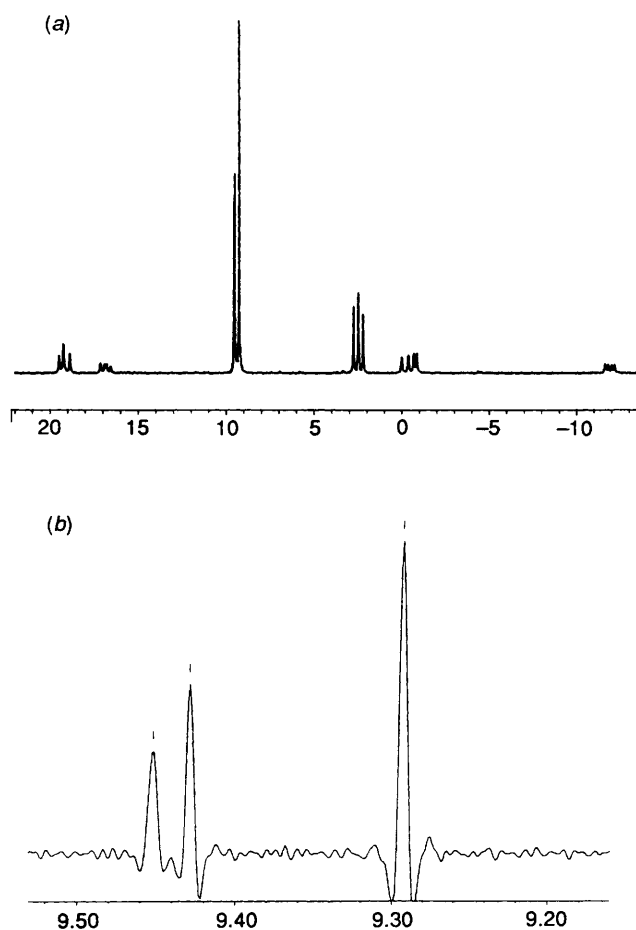


Fig. 5  $^{31}\text{P}\{-^1\text{H}\}$  NMR spectrum of  $[\text{PtCl}(\text{PBu}^n_3)(\text{dppa})]\text{Cl}$  4 at (a) 109.4 MHz and (b) resolution enhanced spectrum at 202.5 MHz

similar cone angles. The chemical shifts of 6–8 show a normal halogen dependence,<sup>26</sup> with increased shielding of the platinum nucleus as the halide becomes heavier. For compound 9 the electronic effects of four co-ordinated phosphorus atoms account for the shift to lower frequency in  $\delta(^{195}\text{Pt})$  relative to the monophosphine complexes, as five-membered chelate rings containing platinum have no significant effect upon  $\delta(^{195}\text{Pt})$  compared with acyclic analogues.<sup>19</sup>

In the  $^1\text{H}$  NMR spectra chemical shift values for the amine proton have previously been reported in only a few cases.<sup>15,17,27–29</sup> The assignment of the resonance due to the NH proton was supported by recording the  $^{195}\text{Pt}$  NMR spectrum of 6 without  $^1\text{H}$  decoupling. Each line in the  $^{195}\text{Pt}$  spectrum is split into a doublet with a coupling found to match that in the  $^1\text{H}$  NMR spectrum for the peak assigned to the amine proton (Fig. 10), suggesting that dissociation of the

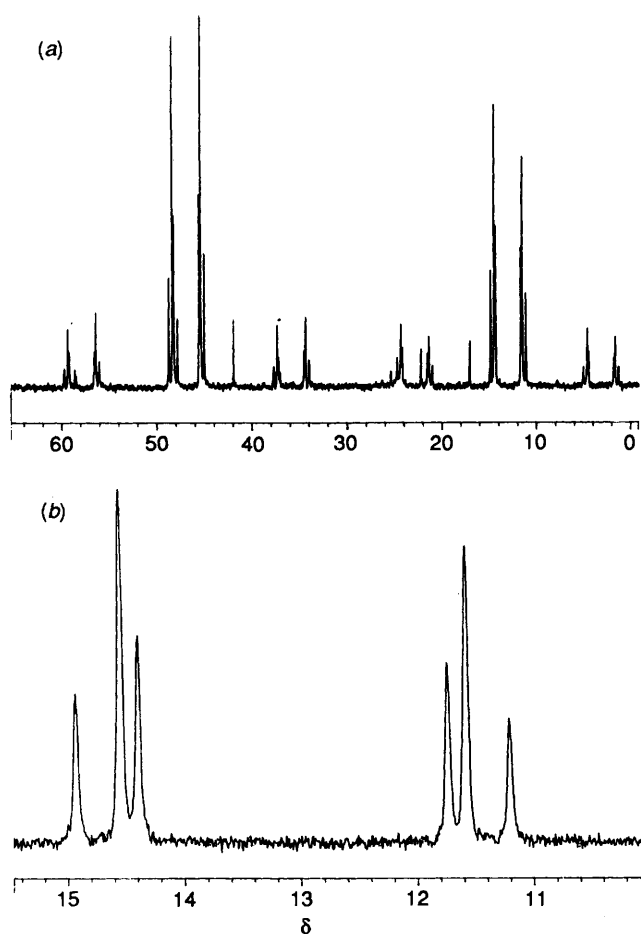


Fig. 6 (a)  $^{31}\text{P}\{-^1\text{H}\}$  NMR spectrum with (b) expansion of the AA' (dppa) region for  $[\text{Pt}(\text{dppe})(\text{dppa})]\text{Cl}_2\cdot\text{CH}_2\text{Cl}_2$  **9**

amine proton from the cationic complex in solution is minimal. The chemical shift of the amine proton in the chloride complexes **1–6** varies little upon changing the monophosphine [ $\delta(\text{NH})$  ca. 11.7,  $^3J(^{195}\text{Pt}-^1\text{H})$  coupling 164–173 Hz]. The deshielding of the NH may, in part, be due to the electron-withdrawing effects of two adjacent co-ordinated phosphorus atoms, as for the free ligand  $\delta(\text{NH})$  is 3.2. The chemical shift of the amine proton in **9** is similar to that for the chloride complexes but  $^3J(\text{Pt}-\text{NH})$  is only 130 Hz. This may arise from the greater *trans* influence of a phosphino group compared to chloride, reducing the Pt–NH coupling through the bond *trans* to it. A similar argument based upon *trans* influence does not hold for the series **6, 7** and **8** where the observed order of  $^3J(\text{Pt}-\text{NH})$  is  $\text{I} > \text{Br} > \text{Cl}$ . Shifts to high frequency for  $\delta(\text{CH}_2)$  in the series  $[\text{Pt}(\text{dppm})_2\text{X}_2]$  ( $\text{X} = \text{Cl}, \text{Br}$  or  $\text{I}$ ) have been attributed to the formation of a five-co-ordinate cationic adduct  $[\text{Pt}(\text{dppm})_2\text{X}]^+$  in solution.<sup>30</sup> Such an interaction of a metal complex with its counter ion is believed to occur in chloroform solution for the structurally similar dppm complex  $[\text{PtCl}(\text{PPh}_2\text{Me})(\text{dppm})]\text{Cl}$ .<sup>24</sup> However, here the fact that the observed shift in  $\delta(\text{NH})$  is to lower frequency may suggest a progressively weaker interaction of the counter ion with the NH group in solution as the halide becomes larger. Coupling of the amine proton to the phosphorus atoms of the dppa ligand is unresolved.

In the IR spectra, as has generally been observed for cationic complexes containing dppa,<sup>5–7,27</sup> there is a significant reduction in  $\nu(\text{N}-\text{H})$  for **1–9** relative to the free ligand ( $3230\text{ cm}^{-1}$ ), due to hydrogen bonding between the NH group and the halide counter ion. The effects of hydrogen bonding upon  $\nu(\text{N}-\text{H})$  is clearly illustrated by the neutral complex **10**, for which such interactions are negligible, where there is a shift to low energy

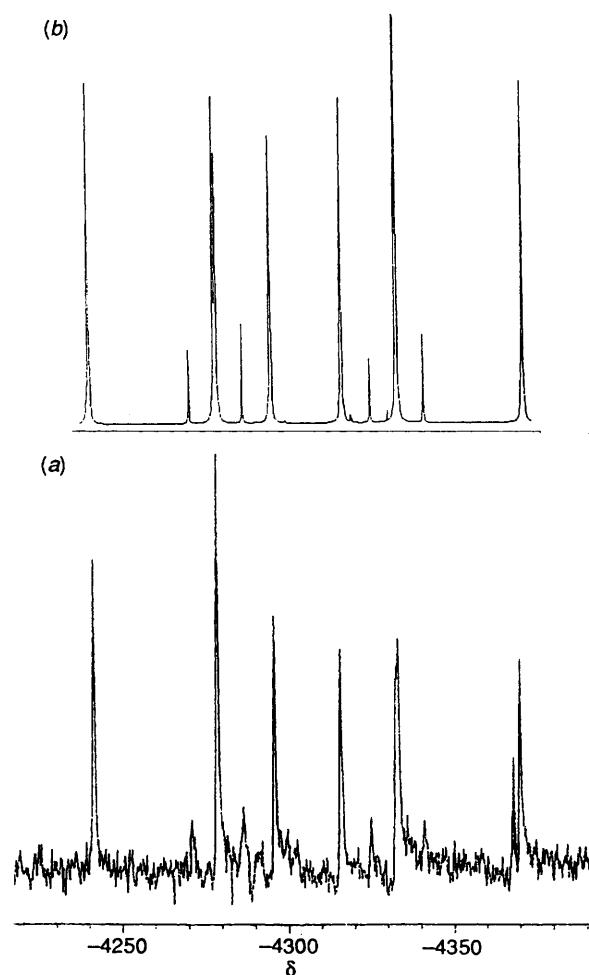


Fig. 7 (a)  $^{195}\text{Pt}\{-^1\text{H}\}$  NMR spectrum and (b) simulation for compound **4**. The small peak at  $\delta -4365$  is due to  $[\text{PtCl}_2(\text{PBu}^n)_2]$  starting material

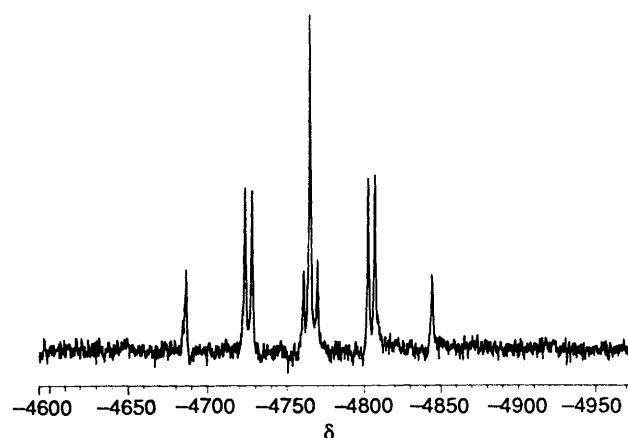


Fig. 8  $^{195}\text{Pt}\{-^1\text{H}\}$  NMR spectrum of compound **9**

of less than  $30\text{ cm}^{-1}$  upon co-ordination. The first overtone of the NH deformation appears as a broad band of similar width and intensity to the NH stretch in the region  $2470\text{--}2530\text{ cm}^{-1}$  for all of the cationic complexes **1–9**.<sup>7</sup> Characteristic bands indicative of chelated dppa appear in the region  $530\text{--}470\text{ cm}^{-1}$ .<sup>5,6</sup> The  $\nu(\text{N}-\text{H})$  and  $2\delta(\text{N}-\text{H})$  bands have a similar line width and intensity, which assists in the identification of the former. The  $\nu(\text{N}-\text{H})$  band moves to higher energy from **6** to **7** to **8** due to diminishing hydrogen-bond strength as the anion becomes larger. For the iodide complex **8** the  $\nu(\text{N}-\text{H})$  and  $2\delta(\text{N}-\text{H})$  bands are sharper than for the corresponding chloride

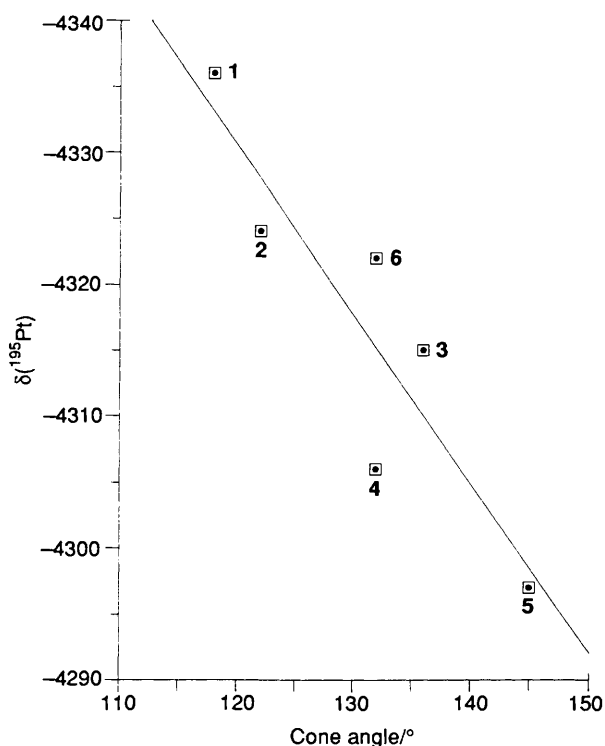


Fig. 9 Plot of  $\delta(^{195}\text{Pt})$  vs. cone angle of phosphine

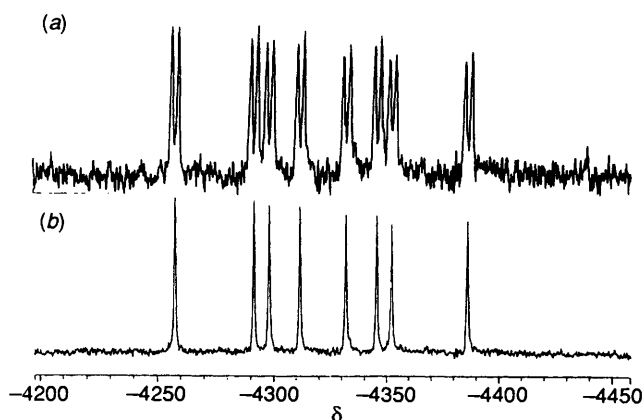


Fig. 10 (a) Undecoupled and (b)  $^1\text{H}$  decoupled  $^{195}\text{Pt}$  NMR spectrum of compound 6

and bromide complexes, confirming the assignment of the band at  $3227\text{ cm}^{-1}$  as the NH stretch of the complex. As mentioned above, the crystal structures of compounds 2, 4 and 9 all show strong N-H...Cl bonds.

The FAB mass spectra of 1-9 confirm their mononuclear nature. For the monophosphine complexes 1-8 the most intense peak in the spectrum corresponds to the parent cation  $[\text{PtX}(\text{PR}_3)(\text{dppa})]^+$  (X = halide). Loss of phosphine follows in all cases to give  $[\text{PtX}(\text{dppa})]^+$ . The most intense peak in the mass spectrum of 9 occurs at  $m/z$  977, indicating the loss of a

proton to give a monocation. The parent dication  $[\text{Pt}(\text{dppe})(\text{dppa})]^{2+}$  gives rise to only a very weak peak at  $m/z$  489.

### Acknowledgements

We are grateful to Johnson Matthey plc for the loan of precious metals.

### References

- 1 R. J. Puddephatt, *Chem. Soc. Rev.*, 1983, 99.
- 2 M. Gomez, G. Muller, J. Sales and X. Solans, *J. Chem. Soc., Dalton Trans.*, 1993, 221.
- 3 R. Rossi, A. Marchi, L. Magon, U. Cassellato, S. Tamburrini and R. Graziani, *J. Chem. Soc., Dalton Trans.*, 1991, 263.
- 4 R. Rossi, A. Marchi, L. Marvelli, M. Peruzzini, U. Cassellato and R. Graziani, *J. Chem. Soc., Dalton Trans.*, 1992, 435.
- 5 R. Uson, J. Fornies, R. Navarro and J. I. Cebollada, *J. Organomet. Chem.*, 1986, 304, 381.
- 6 F. Fornies, R. Navarro and V. Sicilia, *Polyhedron*, 1988, 7, 2659.
- 7 J. Ellermann and L. Mader, *Z. Naturforsch Teil B*, 1980, 35, 307.
- 8 H. Schmidbaur, S. Lauteschlager and B. Milewski-Mahrla, *J. Organomet. Chem.*, 1983, 254, 59.
- 9 N. C. Payne and D. W. Stephan, *J. Organomet. Chem.*, 1981, 221, 203.
- 10 N. C. Payne and D. W. Stephan, *J. Organomet. Chem.*, 1981, 221, 223.
- 11 F. T. Wang, J. Najdzionek, K. L. Leneker, H. Wasserman and D. M. Braitsch, *Synth. React. Inorg. Met. Org. Chem.*, 1978, 8, 119.
- 12 SHELXTL Version 4.2, Siemens Analytical X-Ray Instruments, Madison, WI, 53719, 1990.
- 13 M. T. Costello, D. R. Derringer, P. E. Fanwick, A. C. Price, M. I. Rivera, E. Scheiber, E. W. Siurek III and R. Walton, *Polyhedron*, 1990, 9, 573.
- 14 R. Uson, J. Fornies, R. Navarro, M. Tomas, C. Fortuno, J. I. Cebollada and A. J. Welch, *Polyhedron*, 1989, 8, 1045.
- 15 P. Steil, U. Nagel and W. Beck, *J. Organomet. Chem.*, 1989, 366, 313.
- 16 R. Uson, A. Laguna, M. Laguna, M. Nieves Fraile, P. G. Jones and G. M. Sheldrick, *J. Chem. Soc., Dalton Trans.*, 1986, 291.
- 17 D. R. Derringer, P. E. Fanwick, J. Moran and R. A. Walton, *Inorg. Chem.*, 1989, 28, 1384.
- 18 G. Liehr, G. Szucsanyi and J. Ellermann, *J. Organomet. Chem.*, 1984, 265, 95.
- 19 S. Hietkamp, D. J. Stufkens and K. Vrieze, *J. Organomet. Chem.*, 1979, 169, 107.
- 20 Parameter Adjustment in NMR by Iteration Calculation, Bruker Analytische Messtechnik GMBH, Karlsruhe, 1985.
- 21 *High Resolution NMR; Theory and Chemical Applications*, ed. E. D. Becker, Academic Press, London and New York, 1969.
- 22 P. S. Bratermann, R. J. Cross, Lj. Manojlovic-Muir, K. W. Muir and G. B. Young, *J. Organomet. Chem.*, 1975, 84, C40.
- 23 J. Browning, G. W. Bushnell and K. K. Dixon, *J. Organomet. Chem.*, 1980, 198, C11.
- 24 G. K. Anderson and G. J. Lumetta, *Inorg. Chem.*, 1987, 26, 1518.
- 25 C. A. Tolman, *Chem. Rev.*, 1977, 77, 313.
- 26 *NMR and the Periodic Table*, eds. R. K. Harris and B. E. Mann, Academic Press, London and New York, 1978.
- 27 J. Ellermann, G. Szucsanyi, K. Geibel and E. Wilhelm, *J. Organomet. Chem.*, 1984, 263, 297.
- 28 C. Moreno, M. J. Macazaga and S. Delgado, *J. Organomet. Chem.*, 1990, 397, 93.
- 29 H. Schmidbaur, F. E. Wagner and A. Wohlleben-Hammer, *Chem. Ber.*, 1979, 112, 496.
- 30 M. C. Gossel, R. P. Moulding, K. R. Seddon and F. J. Walker, *J. Chem. Soc., Dalton Trans.*, 1987, 705.

Received 24th February 1993; Paper 3/01109G